

## Gamma-ray resonance study of adsorbed $\text{FeCl}_2$ monolayers\*

Hanan Shechter, J. G. Dash,<sup>†</sup> and M. Mor

*Department of Physics, Technion-Israel Institute of Technology, Haifa, Israel*

R. Ingalls

*Department of Physics, University of Washington, Seattle, Washington 98195*

S. Bukshpan

*Soreg Nuclear Research Center, Yavneh, Israel*

(Received 1 December 1975)

A Mössbauer resonance study of  $\text{FeCl}_2$  monolayers deposited on oriented basal planes of graphite (Grafoil) is reported. Samples with fractional monolayer coverages between 0.2 and 0.9 were studied between 300 and 80°K. The spectra show two distinct quadrupole doublets; one with a room-temperature splitting of  $\sim 2$  mm/sec (designated  $L$ ) and the other  $\sim 0.8$  mm/sec ( $B$ ), which is identical to the splitting of bulk  $\text{FeCl}_2$  and has the same shift. There is a marked difference between the intensities of the two lines of each doublet: For each sample, the ratio  $I_+/I_-$  depends on the orientation of the planes of the Grafoil sheets relative to  $\vec{k}_\gamma$ . The intensity ratio for  $\vec{k}_\gamma$  normal to the plane of the foils progresses from  $I_+/I_- > 1$  to  $I_+/I_- < 1$  with reduction of coverage. The total intensity of the  $B$  doublet relative to  $L$  is reduced with decreasing coverage. The velocity shift of  $L$  and the temperature dependence of the intensity of both  $L$  and  $B$  doublets differ markedly from those of bulk  $\text{FeCl}_2$  and other known  $\text{Fe}^{++}$  compounds. The results suggest the existence of at least two distinct phases of  $\text{FeCl}_2$  in the film samples, and that the  $\text{FeCl}_2$ -graphite samples involve monolayer surface states rather than bulk  $\text{FeCl}_2$  aggregates. A calculation of the adsorption binding energy from the temperature dependence of the Debye-Waller factor yields about 80 kcal/mole for  $B$  and about 60 kcal/mole for the  $L$  phase; both values are larger than the heats of fusion (10 kcal/mole) and evaporation (30 kcal/mole) of bulk  $\text{FeCl}_2$ , and are comparable with the heat of formation (80 kcal/mole). Possible models for surface arrangements of ferrous chloride molecules are discussed.

### I. INTRODUCTION

The physics of systems of dimensionality lower than three has been under increasing interest in recent years, and among the experimental systems studied in this context are adsorbed monolayer films. Various techniques have been newly applied to the study of solid surfaces and adsorbed films, including Mössbauer spectroscopy.<sup>1,2</sup> The Mössbauer technique provides a direct measure of the nuclear mean-squared displacement and internal fields at the resonating nucleus, through which the behavior of the adsorbed molecules can be observed. The principal applications of Mössbauer spectroscopy in surface science have been to problems involving the surface layers of solids, and only a few previous studies of adsorbed monolayers have been reported.<sup>3,4</sup> Unfortunately, there is a difficulty in that there are only two noble-gas isotopes that are suitable for Mössbauer spectroscopy. But it was recently demonstrated<sup>4</sup> that by incorporating  $\gamma$ -active Mössbauer nuclei into large saturated molecules one can in principle use the large variety of Mössbauer resonant isotopes in studies of adsorption. In Ref. 4 the nucleus was  $^{119}\text{Sn}$ ; here we describe a study using  $^{57}\text{Fe}$  in the molecule  $\text{FeCl}_2$ . The substrate in the present study, as in the recent work with  $^{119}\text{Sn}$

compounds, is a commercial form of graphite known as "Grafoil",<sup>5</sup> which presents primarily basal plane exposure for adsorption.

The experimental results are described in Sec. III and in Sec. IV the implications of these results are discussed and related to some possible models describing the arrangements of the  $\text{FeCl}_2$  molecules on the basal plane of the graphite.

### II. EXPERIMENTAL DETAILS

#### A. Samples

Grafoil<sup>5</sup> consists of binderless sheets of expanded graphite crystallites with dominant basal plane orientation parallel to the plane of the sheet. The expansion is produced by treatment in a strongly oxidizing medium such as sulphuric acid and then sudden heating which causes exfoliation. After washing the expanded flakes are rolled into sheets of about 0.3-mm thickness and density less than one-half of bulk crystal. The sheets have large adsorption area due to expansion: Through the thickness of a sheet there are approximately 6000 surfaces open to gas adsorption. Specific area averages to 22 m<sup>2</sup>/g, almost all of which is highly uniform basal plane surface.<sup>6,7</sup> The effective linear dimension of each uniform "domain" is a few hundred Å. Direct measurement of the

orientation distribution has been made by neutron scattering, and shows full width at half-maximum of  $30^\circ$  about the surface normal.<sup>8,9</sup> The preferred orientation is particularly useful in neutron elastic and inelastic scattering by monolayer films<sup>8,9</sup> as well as in the previous studies of physisorption on Grafoil.<sup>3,4</sup> We made use of the preferred orientation in the present study, constructing the sample cells to contain parallel circular discs cut from the Grafoil sheets, so as to orient the average  $c$ -axis direction along the spectrometer axis. The sample cells could also be rotated up to  $50^\circ$  from the parallel direction to examine the orientation dependence of the Mössbauer spectra.

Several sample cells were constructed, all of the same design, each containing ten circular discs of Grafoil in a lightly compressed cylindrical stack. The mass of adsorbent in each stack is about 0.34 g, implying a scaled adsorption area of  $7.6 \text{ m}^2$ . Before loading into a cell each sample was prepared by vapor deposition of a measured quantity of  $\text{FeCl}_2$  single crystal on to the Grafoil by heating together in an evacuated and sealed quartz ampoule. The Grafoil had first been cleaned by baking to  $980^\circ\text{C}$  while pumping in vacuum. After cooling the Grafoil the  $\text{FeCl}_2$  crystal was pushed to the Grafoil zone of the quartz tube and vacuum sealed. After sealing a test was made to check against contamination by distilling the  $\text{FeCl}_2$  from one end of the ampoule to the other by heating to  $780^\circ\text{C}$  and cooling in a temperature gradient. The  $\text{FeCl}_2$  crystallized at the cold end of the ampoule. Visual inspection of color and crystal form was a sensitive check on possible oxidation or hydrolysis. After a satisfactory test the ampoule was heated uniformly to  $750^\circ\text{C}$  (above the sublimation point) and slowly cooled. No traces of  $\text{FeCl}_2$  were then seen, and it was presumed that the material had been deposited uniformly on the substrate by equilibration with the vapor phase. (This presumption was of course subject to consistency tests in the subsequent data analysis, discussed later.) After vapor deposition the capsule was transferred to a dry box filled with  $\text{N}_2$ , broken above a bed of  $\text{P}_2\text{O}_5$  drying agent, and the Grafoil loaded into a sample chamber fitted with Mylar windows. The chamber was then sealed with an indium O-ring gasket and coated with epoxy.

The measured quantities of  $\text{FeCl}_2$  in the samples were 3, 5, 7, and 12 mg, respectively. Together with a thin cleaved crystal of bulk  $\text{FeCl}_2$ , these comprised the five resonant absorbers of this study (see Table I).

#### B. Source

We used a 50-mCi Cu:  $^{57}\text{Co}$  source throughout the experiments.

TABLE I. Resonant absorbers of  $\text{FeCl}_2$  used in the experiments.

Sample	Mass density ( $\text{mg}/\text{m}^2$ )	Fractional monolayer coverage
<i>a</i> , cleaved single crystal	...	...
<i>b</i> , film deposited on Grafoil	1.6	0.9
<i>c</i> , ...	0.9	0.5
<i>d</i> , ...	0.7	0.4
<i>e</i> , ...	0.4	0.2

#### C. Temperature media

A commercial cryo-oven (RICOR MCH-5B)<sup>10</sup> was used. The temperature was regulated by a gold iron versus Chromel-*P* thermocouple, servo controlling the flow of coolant against a heater. The sample temperature could be kept constant within  $\pm 0.05^\circ\text{K}$  during run times. Three gold-plated radiation shields enclosed the sample holder. The windows were made of gold-plated Mylar.

#### D. Spectrometer

An on-line spectrometer operating in a constant acceleration mode accumulated and recorded the velocity spectra. In parallel with the accumulation of the counting rate versus the Doppler velocity spectrum by the computer, the count rate yield of the single-channel pulse-height analyzer was recorded for prefixed scaler clock time so that the 14.4-keV rate could be known for each spectrum and background corrections could be made.

### III. EXPERIMENTAL RESULTS

We obtained the Mössbauer absorption spectrum of each film sample at several temperatures between room temperature and  $80^\circ\text{K}$ . The room temperature results for the monolayer samples and the single crystal are shown in Fig. 1. The single-crystal sample shows the characteristic quadrupole split pattern of bulk  $\text{FeCl}_2$ ,<sup>11-14</sup> with a pronounced asymmetry with intensity ratio  $I_+/I_- = 1.50 \pm 0.07$  for  $\gamma$ -ray transmission parallel to the  $\text{FeCl}_2$   $c$  axis. The expected ratio for a very thin crystal with axial symmetry (field gradient asymmetry parameter  $\eta=0$ ) viewed parallel to the symmetry axis is 3:1. Housley *et al.*<sup>15</sup> have shown that for crystals of finite thickness  $t$  the intensity ratio is substantially smaller than the zero thickness limit. The correct expression for the reduced area,  $I = 2A/\pi f\Gamma$  of a well resolved absorption line with a resonance natural width  $\Gamma$ , is

$$I = \frac{1}{2}c(1+a)\exp[-\frac{1}{2}c(1+a)]I_0[-\frac{1}{2}c(1+a)] + I_1[-\frac{1}{2}c(1+a)] + \frac{1}{2}c(1-a)\exp[-\frac{1}{2}c(1-a)]I_0[-\frac{1}{2}c(1-a)] + I_1[-\frac{1}{2}c(1-a)], \quad (1)$$

where for axial symmetry,  $c_+(\Theta) = [\frac{1}{2} + \frac{1}{8}(3 \cos^2\Theta - 1)]$ ;  $a_+(\Theta) = \sin^2\Theta/(1 + \cos^2\Theta)$ ;  $c_-(\Theta) = [\frac{1}{2} - \frac{1}{8}(3 \cos^2\Theta - 1)]$ ; and  $a_-(\Theta) = 3 \sin^2\Theta/(5 - 3 \cos^2\Theta)$ ;  $A$  is the background corrected experimental area,  $I_0$  and  $I_1$  are the zero- and first-order Bessel functions of imaginary argument.  $c$  is the line intensity function and  $a$  describes the fractional polarization of the line.  $I_+$  is the reduced area of the  $\pm \frac{3}{2} \rightarrow \pm \frac{1}{2}$  transition and  $I_-$  is for the  $\pm \frac{1}{2} \rightarrow \pm \frac{1}{2}$  transition. Our single-crystal sample is of an effective thickness  $t = 3$ . Therefore, for  $\Theta = 0$ ,  $I_+/I_- = 1.51$  which is in agreement with the experimental ratio.

The film spectra are more complicated, showing two main classes of quadrupole doublets; a relatively closely spaced pair which is most strongly

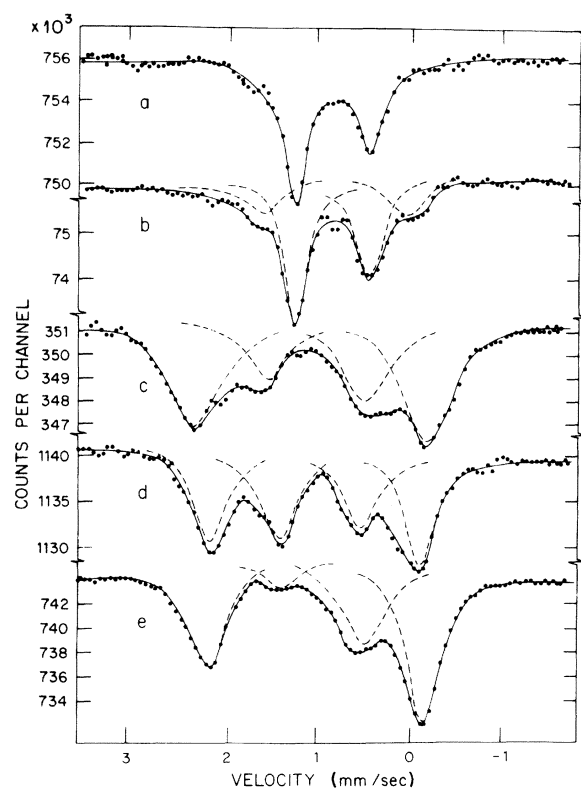


FIG. 1. Resonant spectra of the several  $\text{FeCl}_2$  absorbers at room temperature. (a) Thin cleaved single crystal, with  $\gamma$ -ray wave vector parallel to  $c$  axis; (b) through (e):  $\text{FeCl}_2$  deposited on basal plane graphite, with  $\gamma$ -ray wave vector parallel to the surface normal. The average surface density of each sample is (b)  $1.6 \text{ mg/m}^2$ , (c)  $0.9 \text{ mg/m}^2$ , (d)  $0.7 \text{ mg/m}^2$ , and (e)  $0.4 \text{ mg/m}^2$ , corresponding to fractional monolayer coverages of 0.9, 0.5, 0.4, and 0.2, respectively.

evident in sample  $b$ , and a widely separated doublet that dominates the spectrum of sample  $e$ . These doublets are labeled  $B$  (for its resemblance to the bulk) and  $L$ , respectively. On closer inspection, each sample appears to display both  $B$  and  $L$  spectra, their relative intensities progressing systematically from dominantly  $B$  to dominantly  $L$  with reducing coverage. The intermediate density samples  $c$  and  $d$  have comparable amounts of each type while the extremes have 80% or more of the dominant class. It therefore seems that each film might be composed of two distinct states or phases of  $\text{FeCl}_2$ , with varying concentrations of the phases according to the surface density of the deposit. In the following analysis we present arguments that indicated (i) the  $\text{FeCl}_2$ -graphite samples involve surface states rather than aggregates of bulk ferrous chloride or other iron compounds; (ii) at least two different molecular states are involved in each "B" and "L" spectral class; and (iii) all of the films are monolayers.

The evidence for i includes the magnitude and temperature dependence of the quadrupole splitting, the velocity shift, intensity ratio, and the Debye-Waller factor. The  $B$  pattern of sample  $b$  has the same splitting and velocity shift as bulk  $\text{FeCl}_2$  all the way from room temperature to  $80^\circ\text{K}$ , as shown in Figs. 2 and 3. However, the  $L$  spectrum has a different velocity shift (Fig. 3). The temperature dependence of the intensity for the Grafoil samples ( $L$  and  $B$ ) is different from the bulk  $\text{FeCl}_2$  (Fig. 4): The temperature dependence of the intensity is related to the  $f$  factor, and in Sec. IV it is calculated for samples  $b$  and  $e$  and found to be significantly smaller than the Debye-Waller factor of bulk  $\text{FeCl}_2$ . The  $L$  pattern has a quadrupole splitting comparable to that of hydrated ferrous chloride<sup>16</sup> but it is quite distinctly different in temperature dependence. We also compared the  $L$  splitting and velocity shift with other  $\text{Fe}^{++}$  salts<sup>16</sup> and with amorphous thick films of  $\text{FeCl}_2$ ,<sup>17</sup> and found that the present results are substantially different. Other relevant studies are those of Stukan *et al.*<sup>18</sup> on  $\text{FeCl}_3$ -graphite compounds and successive reduction products: Those results, as well as those reported by Ohhashi *et al.*<sup>19</sup> which will be discussed in more detail later, are similarly distinct from our findings.

The strongest evidence for surface character is the intensity ratio between the components of the doublets, and its dependence on the orientation of the samples with respect to the spectrometer axis. Intensity differences of the two lines of the quad-

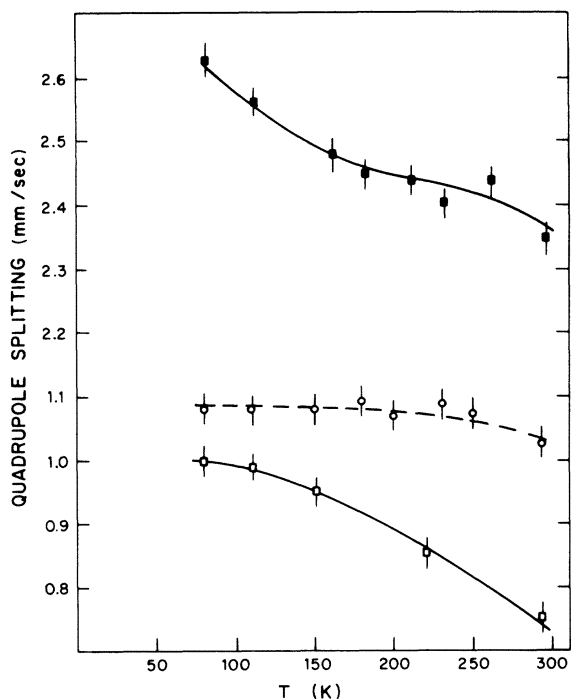


FIG. 2. Quadrupole splitting of several absorbers at various temperatures. Open square, the narrow  $B_1$  doublet of sample  $b$ . The solid line passing through the experimental points corresponds to bulk  $\text{FeCl}_2$ , taken from the data of Ref. 16; open circle, the narrow  $B_2$  doublet of sample  $e$ ; solid square, the wide  $L_2$  doublet of sample  $e$ .

rupole spectrum indicates either a preferred orientation of electric field gradient acting on the nuclei, or in a random distribution of crystallite orientation, a significant anisotropy of the Debye-Waller factor relative to the field gradient direction.<sup>20, 21</sup> In our samples the intensity ratio is associated with the direction of the plane of the Grafoil sheets; this was found by tilting the absorbers up to the maximum possible angle of  $50^\circ$ , which caused the inequality between the line intensities to be markedly reduced. The observed intensity ratio in the  $B_1$  doublet of sample  $b$  is about 1.5:1 when viewed with the plane of the sheets normal to the  $\gamma$ -ray direction. The experimental ratio could be quantitatively analyzed to yield some indication of the distinct character of the film. The effective radiation total thickness of the  $b$  sample is calculated to be  $t=1.2$ , assuming  $f=1$  for both  $B$  and  $L$  components. The relative thickness of the  $B$  phase obtained from the area ratio is 0.9. For this thickness and asymmetry parameter  $\eta=0$  an intensity ratio of  $I_+/I_-=2.1$  is expected [Eq. (1)], which appears to be significantly different from the observations. However, even though we apply a thickness correction for our monolayer sample,

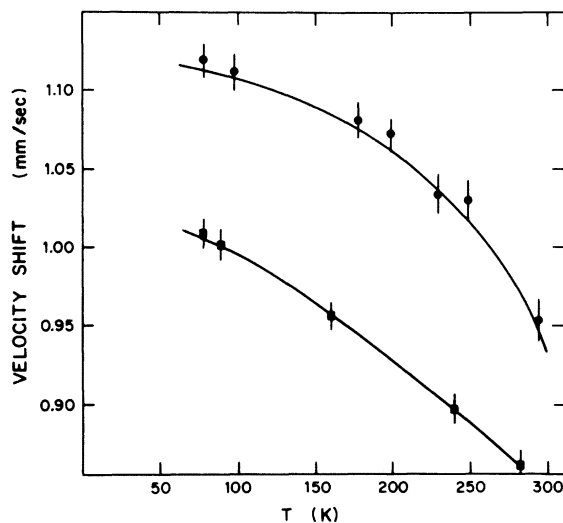


FIG. 3. Velocity shift of the absorption spectra, relative to  $\nu=0$ ; solid square, bulk  $\text{FeCl}_2$  and  $\text{FeCl}_2$  on Grafoil ( $B$ ); solid circle,  $\text{FeCl}_2$ -graphite films,  $L$  spectra.

it may be an irrelevant correction to this particular case since the surface phase arrangement may be different from that of bulk for which the asymmetry parameter is known to be zero. The observed intensity ratio is possibly explained by the observed orientation distribution of  $\sim 30^\circ$  about the surface normal. Together with the finite thickness correction the intensity ratio would be  $\approx 1.77$ . We believe that our result is consistent with this value, within the experimental uncertainty.

In the sequence of spectra (Fig. 1) the intensity ratios of both  $B$  and  $L$  doublets progress from  $I_+/I_- > 1$  to  $I_+/I_- < 1$  with reduction of the quantity of  $\text{FeCl}_2$ . Since the ratio is an indicator of the sign of the field gradient at the nucleus together with its orientation relative to the  $\gamma$ -ray wave vector, the observed sequence shows a series of important changes in either the chemical state or principal orientation of the molecule. Allowing for uncertainties in the measurements, these changes can be modeled by supposing that there are two different phases or subclasses of each class  $B$  and  $L$ , with intensity asymmetries as listed in Table II. The two elements of each class have different quadrupole splittings and shifts;  $B$  is different from  $L$  and similar to the bulk, accounting for appreciable variation in linewidth with coverage and sample temperature.

#### IV. DISCUSSION

We use the Debye-Waller factor and the electric field gradient to characterize our monolayer samples and to help classify some phases.

TABLE II. Four subclasses of quadrupole spectra observed in the experimental film samples, with their characteristic intensity ratios.

Subclass	$B_1$	$B_2$	$L_1$	$L_2$
$I_+/I_-$	$\frac{3}{2}$	$\frac{1}{3}$	1	$\frac{1}{3}$

#### A. Debye-Waller factor

The Debye-Waller factor  $2W$  and Mössbauer fraction  $f = e^{-2W}$  are gauges of the mean squared amplitudes of vibration and force constants of atoms in solids.<sup>22</sup> The importance of  $f$  for surface studies has been emphasized by model calculations.<sup>23,24</sup> The Debye-Waller factor of surface atoms of individual facets of single crystals has been measured by low-energy-electron diffraction,<sup>25</sup> but it is rarely measured in adsorbed films. To our knowledge only two previous studies of adsorbed monolayers<sup>3,4</sup> have successfully yielded values of  $f$ . In the latter the measurements were used as a basis for estimating the binding energy of the adsorbed atoms.<sup>4</sup> In the present study we also estimate the binding energy from the temperature dependence of the intensity (Fig. 4), but use a somewhat different approximation, which we outline below.

The adsorbed molecules are first assumed to be in harmonic vibration normal to the substrate. We postpone a quantitative test of this assumption until the end of the calculation. In all cases of harmonic binding the  $f$  factor for absorption and emission of radiation of wavelength  $\lambda$  by atoms with mean-squared displacement  $\langle(\Delta z)^2\rangle$  is<sup>22</sup>

$$f = \exp[-4\pi^2 \langle(\Delta z)^2\rangle / \lambda^2], \quad (2)$$

where  $z$  is in the direction of propagation of the radiation. Equation (2) is valid for all temperatures. If the atom is vibrating in a discrete mode of frequency  $\omega$  its mean-squared amplitude is given by

$$m\omega^2 \langle(\Delta z)^2\rangle = [\langle n(\omega) \rangle + \frac{1}{2}] \hbar\omega, \quad (3)$$

where  $\langle n(\omega) \rangle$  is the thermal average excitation number, which is governed by the relation

$$\langle n(\omega) \rangle = [\exp(\hbar\omega/k_B T) - 1]^{-1}. \quad (4)$$

Substituting Eqs. (3) and (4) into (2) and taking the derivative with respect to temperature, we obtain

$$-\frac{d \ln f}{dT} = \frac{E_\gamma^2}{mc^2 k_B T^2} \frac{e^x}{(e^x - 1)^2}, \quad (5)$$

where  $x \equiv \hbar\omega/k_B T$ . Equation (5) can be solved explicitly for the frequency

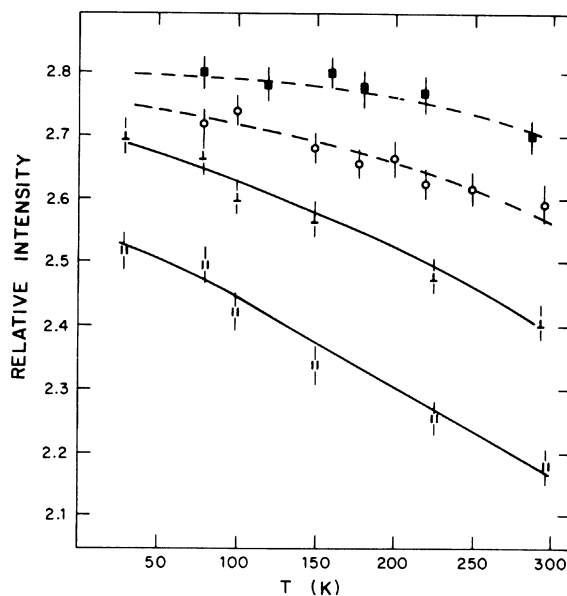


FIG. 4. Relative intensities at various temperatures. Solid square, sample  $b$ , doublet  $B_1$ ; open circle, sample  $e$ , doublet  $L_2$ ;  $\blacktriangle$ , bulk  $\text{FeCl}_2$  along  $c$  axis direction (Ref. 13);  $\parallel$ , bulk  $\text{FeCl}_2$  along layer plane direction (Ref. 13).

$$\frac{\hbar\omega}{k_B T} = 2 \sinh^{-1} \left[ \frac{E_\gamma}{2k_B T} \left( \frac{k_B/mc^2}{-d \ln f/dT} \right)^{1/2} \right], \quad (6)$$

where  $E_\gamma$  is the energy of the  $\gamma$  ray. For moderate to high values of  $f$  ( $\sim 0.5$  to 1) the frequency is primarily dependent on the derivative  $df/dT$  but only weakly dependent on the magnitude of  $f$ . This permits one to extract the desired data from the temperature dependence of the resonant intensity, avoiding the elaborate precautions and instrumental checks which are typically required in absolute  $f$  determinations, which require measurements of the intensity itself.<sup>22</sup> Our estimates of  $df/dT$  for two samples and the corresponding frequency for each are listed in Table III.

To derive the binding energy from the frequency we first make a quadratic fit to the molecule-substrate potential in the region of the minimum. For Van der Waals molecules on smooth Van der Waals

TABLE III. Debye-Waller factors of  $\text{FeCl}_2$  molecules on graphite, and calculated vibration frequencies and binding energies.

Sample and spectral component	$\frac{df}{dT}$ ( $\text{K}^{-1}$ )	$\omega$ ( $\text{sec}^{-1}$ )	$-\epsilon_0$ ( $\frac{\text{kcal}}{\text{mole}}$ )
$b, B_1$	$-5.5 \times 10^{-4}$	$2.4 \times 10^{13}$	79
$e, L_2$	$-8 \times 10^{-4}$	$2.0 \times 10^{13}$	57

solid substrates the interaction has the form<sup>26</sup>

$$\epsilon(z) = A/z^9 - B/z^3, \quad (7)$$

where  $z$  is the distance between the molecule and the surface plane and  $A$  and  $B$  are constants. The energy  $\epsilon_0$  at the minimum can be related to the frequency and the equilibrium separation  $z_0$ :

$$\epsilon_0 = -\frac{1}{27} m\omega^2 z_0^2. \quad (8)$$

To calculate  $\epsilon_0$  we need an independent estimate of  $z_0$ . This can be assumed equivalent to molecules in "contact" with the substrate, using accepted values for the "sizes" of the constituents. For our system we take  $z_0$  to be the sum 3.48 Å of the  $\text{Cl}^-$  ionic radius<sup>27</sup> and one-half of the graphite  $c$ -axis spacing.<sup>28</sup> The resulting values of binding energy are listed in Table III.

The calculated energies are quite large for both samples; about 80 kcal/mole for the close  $B$  doublet of sample  $b$ , and about 60 kcal/mole for the  $L$  doublet of sample 3. Both values are much greater than the heat of fusion (10.3 kcal/mole) and the heat of evaporation (30.2 kcal/mole) of bulk  $\text{FeCl}_2$ ,<sup>29</sup> and the larger value is comparable with the heat of formation of the molecule (81.5 kcal/mole).<sup>30</sup> The fact that they are larger than the heat of evaporation is consistent with their behavior during vapor deposition, since the ferrous chloride evidently deposited in or on the Grafoil in preference to crystallization as bulk crystals even though the substrate was not chilled. The numerical estimate of binding energy is, however, subject to considerable error, as discussed below.

We can first check the validity of the harmonic approximation to the potential of Eq. (7), which depends on the inequality  $\langle (\Delta z)^2 \rangle / z_0^2 \ll 1$ . Using the numerical results we find that the ratio is approximately  $2 \times 10^{-4}$ , and therefore the harmonic approximation is well justified. The overall accuracy of the measurement of  $\epsilon_0$  is probably limited primarily by the uncertainty in  $z_0$  and the approximation of the potential [Eq. (7)] to the actual interaction. There is an appreciable variation in the effective radii of nonmetallic elements in various molecules<sup>31,32</sup> amounting to about 7% in the case of  $\text{Cl}^-$  in molecular crystals; this can cause some 15% error in the estimate of  $\epsilon_0$ . It is more difficult to estimate the uncertainty due to the functional form of Eq. (7), except that we note that in the somewhat parallel case of fitting measured adsorption binding energies to pair potentials the errors can be as great as a factor of 2. However, it seems unlikely that the overall error is so great in our case, for the temperature dependence of the intensity is a direct indicator of stronger binding than in the bulk, while the similarity of the  $B$

spectra to crystalline  $\text{FeCl}_2$  shows that the Fe is in a similar ionic state. Therefore it is our judgment that the material is still chemically  $\text{FeCl}_2$ , i.e., essentially in molecular form, but attached very strongly to the graphite substrate. Recalling the observations of intensity asymmetry described above and its dependence on the angle of the substrate normal with respect to the  $\gamma$ -ray vector, the molecules and/or their field gradient are evidently strongly oriented relative to the substrate plane.

### B. Quadrupole splitting

In the choice of possible phases of  $\text{FeCl}_2$  on Grafoil, the quadrupole splitting may be very helpful. In axial symmetry such as we consider here, this splitting is directly proportional to the magnitude of electric field gradient (EFG) which is given by  $\sum_i z_i \langle (3 \cos^2 \Theta_i - 1) r_i^{-3} \rangle$ . This is a summation over all charges  $z_i$  located at  $r_i$  and  $\Theta_i$  with respect to the nucleus in question,  $\langle \rangle$  denoting expectation value. In ferrous compounds the EFG arises mainly from the  $3d$  electrons in the  $\text{Fe}^{2+}$  ion itself.<sup>12</sup> In spherical or axial symmetry the appropriate one-electron orbital states for these electrons are  $\phi_0 = Y_0^0 f(r)$ ,  $\phi_{\pm 1} = Y_{\pm 1}^{\pm 1} f(r)$ ,  $\phi_{\pm 2} = Y_{\pm 2}^{\pm 2} f(r)$ . Here the  $Y$ 's are spherical harmonics and  $f(r)$  is the appropriate radial wave function. The EFG's are given in units of  $\frac{2}{7} \langle r^{-3} \rangle$ , the appropriate unit for  $d$  wave functions (Table IV).

In the high-spin  $S=2$  state, with five spins up and one spin down, the wave function of the down-spin electron would determine the splitting, since the EFG's from the up spins cancel,<sup>34</sup> and from Table IV, one would expect splittings of one or two units. Qualitatively what is seen in the spectra represented in Fig. 1 somewhat reflects this fact, that is, one has (roughly) two types of splitting, one twice as big as the other. The EFG's also appear to change sign as evidenced by the intensity ratios. To be more specific requires knowledge as to which state, or which combination of states, the minority-spin electron takes. This is determined primarily by the local atomic arrangement. In addition, however, one must con-

TABLE IV. Electric field gradients (efg) from various  $\text{Fe}^{2+}$   $3d$  states. The efg is defined as  $-\langle (3 \cos^2 \Theta - 1) / r^3 \rangle$  and is expressed in units of  $\frac{2}{7} \langle r^{-3} \rangle$  (see text).

State	efg	State	efg
$\phi_0$	-2	$\sqrt{\frac{2}{3}} \phi_{\pm 1} \mp \sqrt{\frac{1}{3}} \phi_{\mp 2}$	0
$\phi_{\pm 1}$	-1	$\sqrt{\frac{2}{3}} \phi_{\pm 2} \mp \sqrt{\frac{1}{3}} \phi_{\mp 1}$	+1
$\phi_{\pm 2}$	+2		

sider the role of temperature, spin-orbit coupling, and other smaller effects.

We shall first discuss the origin of the splitting in bulk  $\text{FeCl}_2$  [Fig. 1(a)] which we find is essentially the same as the main component of the monolayer spectra [Fig. 1(b)]. This will be followed by a tentative interpretation of the several other components observed in this series.

### 1. Splitting in bulk $\text{FeCl}_2$ —and in the nearly completed monolayer on Grafoil

In a lattice of triangular layers, such as bulk  $\text{FeCl}_2$ , the  $\text{Fe}^{2+}$  ion sits at sites of three-fold symmetry. This causes a mixing of  $\phi_{\pm 1}$  with  $\phi_{\mp 2}$ , so that in general one has two doublets  $\phi_H = \cos\theta\phi_{\pm 1} \mp \sin\theta\phi_{\mp 2}$  and  $\phi_L = \cos\theta\phi_{\pm 2} \mp \sin\theta\phi_{\mp 1}$ , and a singlet  $\phi_0$ . If the local symmetry were perfectly octahedral (with the three-fold axis along a [111] direction) then  $\sin\theta = \sqrt{\frac{1}{3}}$  and the respective EFG's for the above states would be 0, +1, -2 units (Table IV). Such is nearly the case for bulk  $\text{FeCl}_2$ , where the octahedron of nearest-neighbor ions is distorted by less than 4% along the octahedron's [111] direction ( $c$  axis). In this approximate octahedral symmetry  $\phi_H$  ( $H$  for "high") lies  $\sim 7000$   $\text{cm}^{-1}$  above  $\phi_L$  ( $L$  for "low") and  $\phi_0$  which are nearly degenerate.<sup>35</sup> If the degeneracy were complete one would expect zero EFG from these states, however from Mössbauer EFG measurements and other studies it is inferred that the doublet  $\phi_L$  is the lowest by  $\sim 100$   $\text{cm}^{-1}$ .<sup>11, 35, 36</sup> However, the reason for this is apparently *not* the slight compression of the octahedron, which would cause  $\phi_0$  to lie lowest, but rather the planar arrangement of the neighboring  $\text{Fe}^{2+}$  ions. Moreover, the latter effect is in turn greatly reduced by the induced dipole moments in the  $\text{Cl}^-$  ions.<sup>37</sup> Thus one has in bulk  $\text{FeCl}_2$ , a, somewhat accidental, near cancellation of the several terms which can remove the degeneracy between electronic levels  $\phi_0$  and  $\phi_L$  and lead to a nuclear quadrupole splitting. If the splitting between  $\phi_0$  and  $\phi_L$  were quite large in comparison to  $\lambda$ , the spin-orbit coupling parameter, ( $\sim 10^2$   $\text{cm}^{-1}$ ) one would expect to see at low temperature a quadrupole splitting of  $\sim 2$  mm/sec or  $\sim 50\%$  of the maximum expected from a  $3d$  state.<sup>12</sup> Instead one observes  $\sim 20\%$ . The high-temperature reduction is of course due to thermal population of  $\phi$ . The intensity ratio for single-crystal  $\text{FeCl}_2$  is also consistent with a positive EFG.

The main component of the nearly completed monolayer spectra of  $\text{FeCl}_2$  on Grafoil, Fig. 1(b), has a splitting essentially identical to the bulk. As mentioned earlier this is extremely strong evidence that one is observing a Cl-Fe-Cl

layered arrangement, much the same as in the bulk. This is entirely consistent with our understanding of the bulk EFG, in that the closest  $\text{Cl}^-$ 's and  $\text{Fe}$ 's can account for the splitting. The intensities of oriented samples are also consistent with a positive EFG.

### 2. Possible origins of the other splittings

As is seen in Fig. 1(b), the nearly completed monolayer has a second component which is weaker and has a larger splitting. At smaller coverages, Fig. 1(c)–(e), an even greater splitting is seen together with small splittings, on the order of that in the bulk. From the present data alone it is not possible to unambiguously derive the structures associated with such splittings. Therefore, we first turn the problem around and ask what possible structures could one have, and how would the splitting vary from structure to structure.

Since the splitting in the bulk and its counterpart in the single monolayer are presumably understood, we shall first consider those structures in registry with the substrate which have this same basic triangular-layer octahedral arrangement with the two  $\text{Cl}^-$  layers remaining in contact. These are shown in Fig. 5 in order of increasing spacing.

As one goes to larger spacings, the splitting between  $\phi_L$  and  $\phi_0$  is expected to first decrease because of the decreased  $\text{Fe}^{2+}$ – $\text{Fe}^{2+}$  interaction which had dominated, and then change sign as the dipole and direct contributions of the more distorted octahedron of  $\text{Cl}^-$  take on more importance. Thus in a phase as described in Fig. 5(a) one expects an EFG more positive than in the bulk, in the 5(b) phase about the same, with phases 5(c) and 5(d) perhaps even smaller. In the formations shown in 5(e) and 5(f) one expects  $\phi_0$  to be below  $\phi_L$  by a small amount leading to negative EFG's which *may* have somewhat greater magnitude than the bulk, however, because of the singlet vs doublet effect.

As the coverage is further lowered one presumably can get away from the double layer of  $\text{Cl}^-$ . A series of single layer  $\text{Cl}^-$  structures may be derived from those above by retaining only the lower layer of  $\text{Cl}^-$  in combination with a honeycomb arrangement of  $\text{Fe}^{2+}$  [Fig. 6(a)]. At bulk spacings one would expect the  $\text{Fe}^{2+}$  contribution to be weakened and  $\phi_0$  lowest yielding a large negative EFG. However as the spacing is increased, the  $\text{Fe}^{2+}$  fits more into the plane and  $\phi_0$  is raised in energy due to its side lobes. In particular with the single layer of  $\text{Cl}^-$  spaced the same in Fig. 5(f) but related to  $\text{Fe}^{2+}$  as in Fig. 6(a) the  $\text{Fe}^{2+}$  would fit

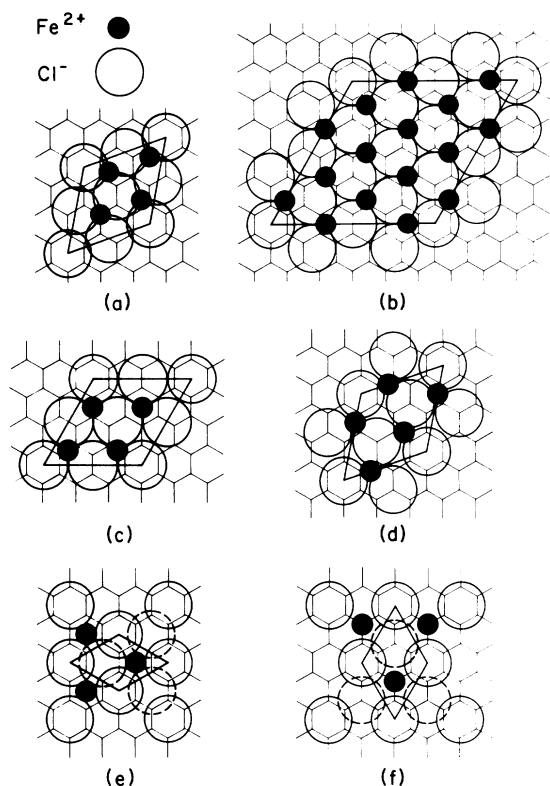


FIG. 5. Possible ordered registered arrangements of octahedrally coordinated  $\text{FeCl}_2$  on Grafoil, (hexagon network) containing two triangular layers of  $\text{Cl}^-$  with a  $\text{Fe}^{2+}$  layer in between. Only in (e) and (f) is the top layer of  $\text{Cl}^-$  pictured (dashed open circles). The horizontal nearest neighbor spacings (in Å) are (a) 3.25, (b) 3.55, (c) 3.69, (d) 3.76, (e) 4.26, and (f) 4.92. The bulk spacing is 3.58.

nicely in the plane and one would expect  $\phi_L$  to again be lowest, producing a positive EFG, greater than in the bulk.

A third possible series of structures would comprise planar arrangements of linear  $\text{FeCl}_2$  molecules (Fig. 7). The graphite spacing is about right to accommodate such an arrangement. Regarding the  $z$  axis to lie along the Cl-Fe-Cl axis one expects  $\phi_{\pm 2}$  to lie lowest, producing a large positive EFG. When viewed from above the plane, i.e., perpendicular to this axis, one then expects an intensity ratio of the spectra similar to that along the axis of a negative EFG (i.e., inner line more intense). The situation will probably not be substantially different whether such linear molecules are isolated or packed in one of the many possible ordered or disordered arrangements.

We also consider two additional structures which are somewhat distinct from the octahedral type of Fig. 5, triangular layer of Fig. 6(a), or molecular of Fig. 7. The first (not pictured) would be essen-

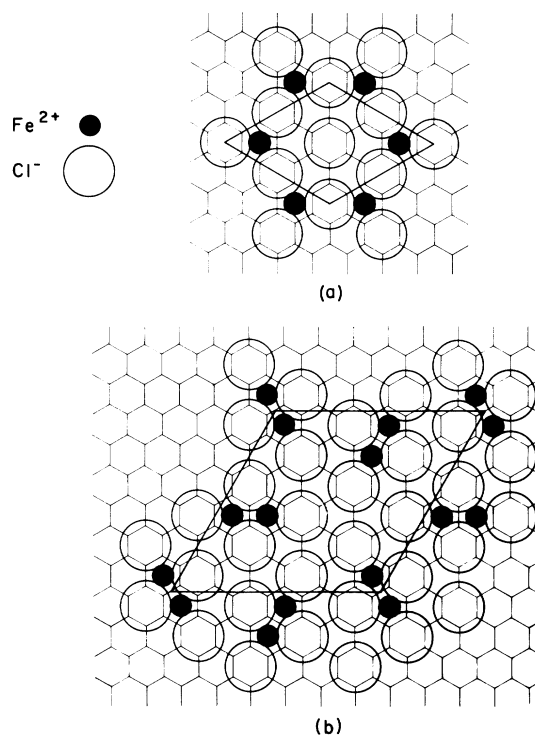


FIG. 6. Possible ordered registered arrangements of  $\text{FeCl}_2$  on Grafoil: (a) Honeycomb arrangement of  $\text{Fe}^{2+}$  coupled with triangular  $\text{Cl}^-$  structure; (b) an arrangement of dimers with  $\text{Cl}^-$  in a  $\sqrt{3} \times \sqrt{3}$  configuration.

tially the same as in Fig. 5(e) or 5(f) with the second layer of  $\text{Cl}^-$  directly above the  $\text{Fe}^{2+}$  ions which now fit below in between the lower  $\text{Cl}^-$ 's and may be somewhat bonded to the graphite. The second [Fig. 6(b)] is an ordered or disordered arrangements of dimers, that is, the  $\text{Cl}^-$  as in Fig. 6(a) but with the  $\text{Fe}^{2+}$  pairing. Such a structure has been proposed for  $\text{Be}_2\text{Cl}_4$ .<sup>38</sup> Dimers are known to

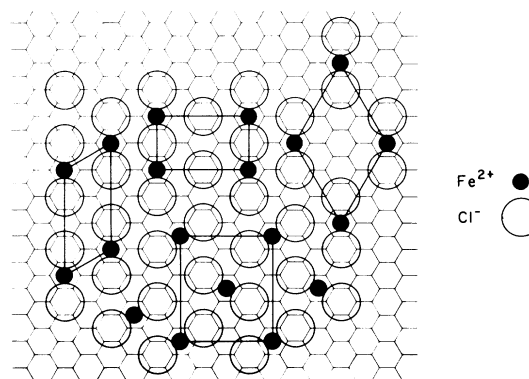


FIG. 7. Various possible unit cells for arrangements of  $\text{FeCl}_2$  monomers in Grafoil with the  $\text{Cl}^-$  in  $2 \times 2$  configuration. (See Fig. 5 for notation.)



be present in  $\text{FeCl}_2$  vapor.<sup>39</sup> Here extra stabilization may occur if one  $\text{Fe}^{2+}$  is above the  $\text{Cl}^-$  plane and the other is below. The splittings from these two structures are less easily calculated but appear to be of intermediate strength with either sign of the EFG possible.

### 3. Discussion and criticism of the suggested phases

As stated in Sec. IV B 2 it is not possible to calculate the quadrupole splitting associated with the many possible structures with sufficient accuracy to compare quantitatively with experiment. Even for the bulk case, problems of covalency and the strength of the induced  $\text{Cl}^-$  dipole moment make reliable first principles calculations of both the  $\phi_o - \phi_L$  separation  $\Delta$  and the resulting EFG impossible. Moreover, a unique set of parameters such as  $\lambda$ ,  $\Delta$ , and  $\langle r^{-3} \rangle$  is also not perfectly obtainable from the data. For example, Hazony and Ok<sup>35</sup> deduce  $\Delta \sim 340 \text{ cm}^{-1}$ , while Alben<sup>36</sup> chooses  $\sim 90 \text{ cm}^{-1}$ . Even if one could properly treat the problem of the Fe-Cl interaction and apply it to the suggested layer arrangements, it would not be too surprising if the graphite were to modify  $\Delta$  sufficiently to affect the calculated quadrupole splittings. Therefore although in this section we return to the measurements, one must bear in mind these problems.

It is very likely that the narrow doublet that persists throughout the spectra is from the bulklike layer phase as discussed in Fig. 1 above. Even in the less dense phases it would not be too unlikely for the linear  $\text{FeCl}_2$  molecules to cluster together in this form. One cannot absolutely rule out structures such as Figs. 5(b)–(d), although it would be quite accidental if they were to give the precise bulk splitting. The structure shown in Fig. 5(a) seems too compressed to be a viable choice.

It is possible but unlikely that one of the former structures could even account for the second component of the dense layer spectrum [Fig. 1(b)], which also seems present in the less dense cases [Fig. 1(c)–(e)]. Indeed spectra similar to Fig. 1(b) have been obtained by Ohhashi and Tsujikawa<sup>19</sup> for  $\text{FeCl}_2$  intercalated in graphite. In that case the  $\text{FeCl}_2$  had the bulk spacing but was in partial registry, in the sense that the  $\text{FeCl}_2$  and graphite  $a$  axes were parallel. Moreover, there were two Fe sites in the ratio of  $\sim 2$  to 1, with the less populated site presumably distorted enough to produce the enlarged splitting. In that case it was not clearly indicated how such a situation could come about, however. None of our suggested structures satisfy all these requirements. Figure 5(c) does have an  $a$  axis parallel to the substrate, but  $a$  is too large and there is only one Fe site. Figure

5(d) has two Fe sites, but in the ratio 3:1; moreover, the  $a$  axis is rotated and the wrong length, etc. We also expect smaller splittings from Figs. 5(c) and 5(d) rather than larger. Moreover, this intermediate splitting is different from that of Ref. 19 at low temperature, and exhibits no appreciable asymmetry.

We feel it is more likely that this intermediate component comes from a structure like 5(e): Such a structure has in fact been observed in the case of  $\text{GeI}_2$  on graphite.<sup>40</sup> It would have 0.7 times the density of a bulk-type layer and would be expected to produce a negative EFG of roughly the same or larger magnitude. There are, of course, a number of other structures that may give such intermediate splitting. Those shown in Figs. 5(c) and 5(d) probably would give a smaller splitting than the  $B$  spectra. However, larger splittings could instead result because of the lack of axial symmetry about the iron site. The structures of Fig. 6 are also reasonable possibilities. The dimer arrangement of Fig. 6(b) may either form from deposition of dimers or else come from a condensation of deposited monomers such as in Fig. 7. The arrangement on Fig. 6(a) [with the same Cl spacing as in Fig. 5(e)] could conceivably come from Fig. 6(b) by a hopping of the Fe ions. A similar arrangement to Fig. 6(a) but with, for example, the bulk Cl spacing seems less likely to form and is expected to yield too large a splitting. Final possibilities for the intermediate splitting would be like in Fig. 5(f) [or possibly Fig. 5(e)] but with the upper layer of Cl ions directly on the Fe ions.

For reasons stated earlier, some of the above structures can not even be completely ruled out as far as producing the largest splitting ( $L$ ) in the spectra 1(c), 1(d), and 1(e). However, we feel that it is far more likely that this component derives from one of many planar arrangements of the linear molecules such as in Fig. 7, all of which are expected to yield about the same splitting.

One possible problem with such an interpretation lies with an earlier Mössbauer measurement of  $\text{FeCl}_2$  isolated in frozen rare-gas matrices.<sup>41</sup> There a rather small splitting and isomer shift were obtained, as compared with the bulk. It is generally agreed in the literature that the ground state of the linear  $\text{FeCl}_2$  molecules should be essentially  $\phi_{\pm 2}$ . We have made rough estimates of the reduction effects of covalency on the quadrupole splitting and isomer shift for this case and believe such effects to be *smaller* than in the bulk. Essentially this is because of less overlap with the  $2p$  wave functions of the  $\text{Cl}^-$ . That is, one expects a large splitting and shift, just what we observe in our experiment. The same reasoning (i.e., reduced overlap) may explain why all the

components other than those attributed to the "bulk" arrangements have larger isomer shifts. Therefore it is quite likely that the rare-gas matrix has significantly affected the electronic structure of the  $\text{FeCl}_2$  molecules in the matrix isolation experiments.

### V. SUMMARY

In the attempt to identify the several molecular states in our samples, we find the clearest indications in sample *b*. We believe it consists primarily of  $\text{FeCl}_2$  monolayers deposited on the basal plane graphite surfaces of the Grafoil. The velocity shift, quadrupole splitting, and intensity asymmetry of its principal spectral component ( $B_1$ ) is the same as a single crystal of  $\text{FeCl}_2$  viewed along the *c* axis, whereas the recoilless fraction is different. It is plausible that the difference in temperature dependence of the intensity can be accounted for by the strong binding to the graphite. The strong binding, deduced from the recoilless fraction, is consistent with the adsorptive properties of basal plane graphite for many Van der Waals molecules.<sup>6-9, 26, 33, 42</sup> This binding is plausibly stronger than that between the layers of  $\text{FeCl}_2$  in the bulk crystal, which are also of the Van der Waals type, for on the basis of simple scaling procedures<sup>38, 39</sup> the  $\text{FeCl}_2$ -graphite interaction is stronger than  $\text{FeCl}_2$ - $\text{FeCl}_2$ . The density of deposit is consistent with these conclusions; a single layer of  $\text{FeCl}_2$  of the bulk crystal structure spread uniformly on the total adsorption area of the Grafoil would have areal density  $1.87 \text{ mg/m}^2$ , which is approximately equal to the average density  $1.6 \text{ mg/m}^2$  of sample *b*. In the recent study of Stukan, *et al.*,<sup>18</sup> a related structure was deduced: single layers of  $\text{FeCl}_2$  alternating with graphite planes. This arrangement is one of a large number of graphite layer compounds that can be formed by intercalating graphite with various chemicals.<sup>43</sup> Stukan *et al.* and later Ohhashi *et al.*<sup>19</sup> formed the  $\text{FeCl}_2$ -graphite compound by first intercalating  $\text{FeCl}_3$  into graphite and then reducing it. This procedure had to be followed since  $\text{FeCl}_2$  is not among the chemicals that can be intercalated directly into graphite. This is an

important point in regard to our study, guaranteeing that the  $\text{FeCl}_2$  in the Grafoil was deposited only on the already exposed surfaces of the exfoliated graphite sheets and not between the atomic layers of the unexfoliated crystals. A further important point is that in the intercalated graphite compounds the  $\text{FeCl}_2$  evidently retained its form in the intermediate reduction products, thus it can exist in undissociated molecules in spite of its strong interaction with the graphite layers. All of the above indications combine to give a persuasive identification of the dominant  $B_1$  phase of sample *b*, as a single molecular layer of bulk  $\text{FeCl}_2$ , oriented with its *c* axis normal to the surface plane.

In this study we have tried to demonstrate the capability of the Mössbauer spectroscopy for studies of adsorbed monolayer films. We used the hyperfine interaction on the Mössbauer nucleus to attempt to distinguish among various surface phases. The Debye-Waller factor was used as an indicator of the strength of the monolayer bond to the substrate as compared with that of the bulk. Although the present study is quite detailed in several respects, much more extensive examinations are needed for complete analysis. We did not measure the *f* factor parallel to the graphite basal plane, due to technical difficulties. The difficulties of sample preparation prevented us from preparing a substantially larger number of samples. It was therefore impossible to study surface phase transitions. In the present study, we did not observe any gross change in  $\langle(\Delta z)^2\rangle_T$  in the experimental temperature range. It would be interesting to compare intensities for possible changes in  $f_{\parallel}$  (changes on the surface) relative to  $f_{\perp}$  (perpendicular to the surface); such changes should be associated with possible phase transition, which should cause  $f_{\parallel}$  to decrease while  $f_{\perp}$  should remain insensitive to temperature changes. From this viewpoint it would be interesting to study an iron compound with a convenient room-temperature vapor pressure; this may enable one to follow and control changes in coverage and to follow the responses of the Mössbauer spectra, with a sample chamber in the observing position at all times. Attempts are being done in this direction.

\*Sponsored by the Israel-U.S. Binational Science Foundation.

†On leave from the Physics Dept., University of Washington, Seattle, Wash.

<sup>1</sup>M. J. D. Low, *The Solid-Gas Interface*, Vol. 1, edited by E. A. Flood (Dekker, New York, 1966).

<sup>2</sup>M. C. Hobson, Jr., *Characterization of Solid Surfaces*,

edited by P. F. Kane and G. B. Larrabee (Plenum, New York, 1974), Chap. 15.

<sup>3</sup>S. Bukshpan and S. L. Ruby, *Bull. Am. Phys. Soc.* **16**, 850 (1971).

<sup>4</sup>S. Bukshpan, T. Sonnino, and J. G. Dash, *Surf. Sci.* **54**, 466 (1975).

<sup>5</sup>Grafoil is a commercial product marketed by Union

- Carbide Corp., Carbon Products Div., 270 Park Ave., New York.
- <sup>6</sup>M. Bretz, J. G. Dash, D. C. Hickernell, E. O. McLean, and O. E. Vilches, *Phys. Rev. A* **8**, 1589 (1973); **9**, 2814 (1974).
- <sup>7</sup>R. L. Elgin and D. L. Goodstein, *Phys. Rev. A* **9**, 265 (1974).
- <sup>8</sup>J. K. Kjems, L. Passell, H. Taub, and J. G. Dash, *Phys. Rev. Lett.* **32**, 724 (1974).
- <sup>9</sup>J. K. Kjems, L. Passell, H. Taub, J. G. Dash, and A. D. Novaco, *Phys. Rev. B* **13**, 1446 (1976).
- <sup>10</sup>"RICOR" Ltd., Cryogenic and Vacuum Systems, En Harod (Ihud), Israel.
- <sup>11</sup>K. Ôno, A. Ito, and T. Fujita, *J. Phys. Soc. Jpn.* **19**, 2119 (1964).
- <sup>12</sup>R. Ingalls, *Phys. Rev.* **121**, 63 (1961).
- <sup>13</sup>D. P. Johnson and J. G. Dash, *Phys. Rev.* **172**, 983 (1968).
- <sup>14</sup>H. K. Perkins and Y. Hazony, *Phys. Rev. B* **5**, 7 (1972).
- <sup>15</sup>R. M. Housley, U. Gonser, and R. W. Grant, *Phys. Rev. Lett.* **20**, 1279 (1968).
- <sup>16</sup>*Mössbauer Effect Data Index, 1968-1971*, edited by J. G. Stevens and V. E. Stevens (Plenum, New York, 1970-1972).
- <sup>17</sup>A. J. F. Boyle, G. M. Gruen, J. R. Clifton, and R. L. McBeth, *J. Phys. (Paris)* **32**, Suppl. C1-224 (1971).
- <sup>18</sup>R. A. Stukan, V. A. Prusakov, Yu. N. Novikov, M. E. Volpin and V. I. Goldanskii, *Zh. Strukt. Khim.* **12**, 622 (1971) [*J. Struct. Chem. USSR* **12**, 567 (1971)] [(Consultants Bureau, 227 W. 17th St., New York)].
- <sup>19</sup>K. Ohhashi, and I. Tsujikawa, *J. Phys. Soc. Jpn.* **37**, 63 (1974).
- <sup>20</sup>R. W. Grant, in *Mössbauer Effect Methodology*, Vol. 2, edited by I. J. Gruverman (Plenum, New York, 1966), pp. 23-38.
- <sup>21</sup>R. L. Collins and J. C. Travis, in Ref. 20, Vol. 3, pp. 123-162.
- <sup>22</sup>R. H. Nussbaum, in Ref. 20, Vol. 2, pp. 3-21.
- <sup>23</sup>A. A. Maradudin and J. Melngailis, *Phys. Rev.* **133**, A1188 (1964).
- <sup>24</sup>R. E. Allen and F. W. de Wette, *J. Chem. Phys.* **54**, 2605 (1971).
- <sup>25</sup>M. W. Webb and M. G. Lagally, *Solid State Phys.* **28**, 302 (1973).
- <sup>26</sup>J. G. Dash, *Films on Solid Surfaces* (Academic, New York, 1975).
- <sup>27</sup>L. Pauling, *The Nature of the Chemical Bond* (Cornell U.P., Ithaca, N.Y., 1960).
- <sup>28</sup>Y. Baskin and L. Meyer, *Phys. Rev.* **100**, 544 (1955).
- <sup>29</sup>D. Nicholas, *Comprehensive Inorganic Chemistry*, Vol. 3 (Pergamon, New York, 1973), p. 979.
- <sup>30</sup>V. I. Vedeneyev, L. V. Gurvich, V. N. Kondratyev, V. A. Medvedev, and Ye. L. Frandevich, *Bond Energies, Ionization Potentials, and Electron Affinities* (Arnold, London, 1966).
- <sup>31</sup>A. Bondi, *J. Phys. Chem.* **68**, 441 (1964).
- <sup>32</sup>*Tables of Interatomic Distances in Molecules and Ions*, Spec. Publ. No. 18 (Chemical Society, London, 1958, 1965), Suppl.
- <sup>33</sup>A. D. Crowell and W. A. Steele, *J. Chem. Phys.* **34**, 1347 (1961).
- <sup>34</sup>This neglects covalent effects and assumes  $\langle r^{-3} \rangle$  is the same from all states.
- <sup>35</sup>Y. Hazony and H. N. Ok, *Phys. Rev.* **188**, 591 (1969).
- <sup>36</sup>R. Alben, *J. Phys. Soc. Jpn.* **26**, 261 (1969).
- <sup>37</sup>J. Kanamori, *Prog. Theor. Phys.* **20**, 890 (1958).
- <sup>38</sup>A. Büchler and W. Klemperer, *J. Chem. Phys.* **29**, 121 (1958).
- <sup>39</sup>C. W. DeKock and D. M. Gruen, *J. Chem. Phys.* **44**, 4387 (1960); G. E. Loroi, *ibid.* **36**, 2879 (1963).
- <sup>40</sup>J. J. Lander and J. Morrison, *Surf. Sci.* **6**, 1 (1967).
- <sup>41</sup>T. K. McNab, D. H. W. Carstens, D. M. Gruen, and R. L. McBeth, *Chem. Phys. Lett.* **13**, 600 (1972).
- <sup>42</sup>W. A. Steele and R. Karl, *J. Colloid Interface Sci.* **28**, 397 (1968).
- <sup>43</sup>A. R. Ubbelohde and F. A. Lewis, *Graphite and its Crystal Compounds* (Oxford U.P., Oxford, 1960).